

Measuring diffusion with polarization-modulation dual-focus fluorescence correlation spectroscopy

You Korlann¹, Thomas Dertinger¹, Xavier Michalet¹,
Shimon Weiss¹, Jörg Enderlein^{2*}

¹UCLA, Department of Chemistry and Biochemistry, University of California, Los Angeles, CA 90095, USA

²Institute for Physical and Theoretical Chemistry, Eberhard Karls University Tübingen,
D-72076 Tübingen, Germany

*Corresponding authors: joerg.enderlein@uni-tuebingen.de

Abstract: We present a new technique, polarization-modulation dual-focus fluorescence correlation spectroscopy (pmFCS), based on the recently introduced dual-focus fluorescence correlation spectroscopy (2fFCS) to measure the absolute value of diffusion coefficients of fluorescent molecules at pico- to nanomolar concentrations. Analogous to 2fFCS, the new technique is robust against optical saturation in yielding correct values of the diffusion coefficient. This is in stark contrast to conventional FCS where optical saturation leads to an apparent decrease in the determined diffusion coefficient with increasing excitation power. However, compared to 2fFCS, the new technique is simpler to implement into a conventional confocal microscope setup and is compatible with cw-excitation, only needing as add-ons an electro-optical modulator and a differential interference contrast prism. With pmFCS, the measured diffusion coefficient (D) for Atto655 maleimide in water at 25°C is determined to be equal to $(4.09 \pm 0.07) \times 10^{-6} \text{cm}^2/\text{s}$, in good agreement with the value of $4.04 \times 10^{-6} \text{cm}^2/\text{s}$ as measured by 2fFCS.

©2008 Optical Society of America

OCIS codes: (170.6280) Spectroscopy, fluorescence and luminescence; (180.1790) Confocal Microscopy; (300.2530) Fluorescence, laser-induced.

References

1. A. Einstein, *Investigations on the theory of the Brownian movement* (Dover Publications, New York, 1956), p. 119 p.
2. D. Magde, E. Elson, and W. W. Webb, "Thermodynamic Fluctuations in a Reacting Systems - Measurement by Fluorescence Correlation Spectroscopy," *Phys. Rev. Lett.* **29**, 705 (1972).
3. D. M. Elliot L. Elson, "Fluorescence correlation spectroscopy. I. Conceptual basis and theory," *Biopolymers* **13**, 1-27 (1974).
4. D. Magde, E. L. Elson, and W. W. Webb, "Fluorescence correlation spectroscopy. II. An experimental realization," *Biopolymers* **13**, 29-61 (1974).
5. J. Enderlein, I. Gregor, D. Patra, and J. Fitter, "Art and artefacts of fluorescence correlation spectroscopy," *Curr. Pharm. Biotechnol.* **5**, 155-161 (2004).
6. J. Enderlein, I. Gregor, D. Patra, T. Dertinger, and U. B. Kaupp, "Performance of fluorescence correlation spectroscopy for measuring diffusion and concentration," *ChemPhysChem* **6**, 2324-2336 (2005).
7. K. Berland and G. Shen, "Excitation saturation in two-photon fluorescence correlation spectroscopy," *Appl. Opt.* **42**, 5566-5576 (2003).
8. G. Nishimura and M. Kinjo, "Systematic error in fluorescence correlation measurements identified by a simple saturation model of fluorescence," *Anal. Chem.* **76**, 1963-1970 (2004).
9. I. Gregor, D. Patra, and J. Enderlein, "Optical saturation in fluorescence correlation spectroscopy under continuous-wave and pulsed excitation," *ChemPhysChem* **6**, 164-170 (2005).

10. T. Dertinger, V. Pacheco, I. von der Hocht, R. Hartmann, I. Gregor, and J. Enderlein, "Two-focus fluorescence correlation spectroscopy: a new tool for accurate and absolute diffusion measurements," *ChemPhysChem* **8**, 433-443 (2007).
11. B. K. Müller, E. Zaychikov, C. Bräuchle, and D. C. Lamb, "Pulsed interleaved excitation," *Biophys. J.* **89**, 3508-3522 (2005).
12. D. V. O'Connor and D. Phillips, *Time-correlated single photon counting* (Academic Press, London ; Orlando, 1984), pp. viii, 288 p.
13. C. B. Müller, K. Weiß, W. Richtering, A. Loman, and J. Enderlein, "Calibrating Differential Interference Contrast Microscopy with dual-focus Fluorescence Correlation Spectroscopy," *Opt. Expr.* **16**, 4322-4329 (2008).
14. K. Schätzel, *Single Photon Correlation Techniques. Dynamic Light Scattering: The method and some applications* (Clarendon Press, Oxford, 1993).

1. Introduction

Precise diffusion measurement of biomolecules at pico- to nanomolar concentrations is a difficult but important task with many potential applications. The diffusion coefficient of a molecule is directly related to its hydrodynamic radius via the famous Stokes-Einstein relation [1]. Any change in that radius will change the associated diffusion coefficient of the molecules. Such changes occur to most biomolecules – in particular proteins, RNA and DNA – when interacting with their environment (e.g., binding of ions or other biomolecules) or performing biologically important functions (e.g., enzymatic catalysis) or reacting to changes in environmental parameters such as pH, temperature, solvation (e.g. protein unfolding) etc. A standard method for measuring the diffusion at low concentrations is to label the molecules of interest with fluorescent marker and to perform a fluorescence correlation spectroscopy (FCS) measurement [2-4]. Because the temporal decay of the measured autocorrelation function (ACF) is related to the diffusion speed of the molecules, one can, in principle, extract from an FCS experiment the diffusion coefficient and thus hydrodynamic radius of the diffusing molecules. However, to extract a correct value of the diffusion coefficient from an FCS measurement, one needs precise knowledge of the shape and size of the detection volume or, more precisely, the molecule detection function (MDF) that describes the position-dependent probability to excite and detect a fluorescence photon from a molecule at a given position within the sample. In practice, the MDF is poorly known and subject to many specificities and conditions of the measurement such as cover slide thickness variation, refractive index mismatch, or laser beam characteristics, see, e.g., [5, 6]. One of the most disturbing observations is the dependence of the measured ACF on excitation intensity due to optical saturation of fluorescence which is observed even at very low total excitation power [7-9]. This makes even comparative measurements problematic, because the photophysics and thus optical saturation properties of fluorescent labels often change when they are chemically bound to a target molecule.

Recently, a new method, dual-focus FCS (2fFCS) was introduced to circumvent all the above mentioned problems of conventional FCS [10]. The core idea is to generate two overlapping foci with *precisely know distance* between them. Instead of measuring only the ACF of the signal originating from a single focus, one measures the ACF of the signal originating from each focus, and the cross-correlation function (CCF) of the signals from both foci. By globally fitting all three curves and knowing the exact distance between foci, it is possible to extract a correct value of the diffusion coefficient even in the presence of considerable optical aberrations or optical saturation of the fluorescence. The achievable accuracy of the method was shown to be better than 5 % in absolute value.

The original 2fFCS set-up used two pulsed (50 ps pulse width, 40 MHz overall repetition rate), spectrally identical lasers for generating the two foci, and employed pulsed interleaved excitation (PIE) [11] and time-correlated single-photon counting (TCSPC) [12] to temporally distinguish the fluorescence signals originating from each focus. Although this technique

works exceptionally well, one needs an expensive pulse-interleaved laser excitation system and TCSPC detection electronics and signal processing, which restricts the wider dissemination of the 2fFCS idea to existing FCS set-ups employing single laser cw-excitation without TCSPC capabilities. Here, we modify the general idea of 2fFCS in such a way that it can be used also with standard cw-excitation and standard correlation hardware and/or software. We demonstrate the technique by measuring the diffusion coefficient of a reference dye with known diffusion coefficient, and compare the result with results of 2fFCS using PIE.

2. Theory and data analysis

As was shown in Ref. [10], an appropriate model function for the MDF of a confocal microscope is given by

$$U(\mathbf{r}) = \frac{\kappa(z)}{w^2(z)} \exp\left[-\frac{2}{w^2(z)}(x^2 + y^2)\right] \quad (1)$$

where x and y are transversal coordinates perpendicular to the optical axis $z = 0$, and the functions $\kappa(z)$ and $w(z)$ are given by

$$w(z) = w_0 \left[1 + \left(\frac{\lambda_{ex} z}{\pi w_0^2 n} \right)^2 \right]^{1/2} \quad (2)$$

and

$$\kappa(z) = 2 \int_0^a \frac{d\rho\rho}{R^2(z)} \exp\left(-\frac{2\rho^2}{R^2(z)}\right) = 1 - \exp\left(-\frac{2a^2}{R^2(z)}\right) \quad (3)$$

where the function $R(z)$ is defined by an expression similar to Eq.(2):

$$R(z) = R_0 \left[1 + \left(\frac{\lambda_{em} z}{\pi R_0^2 n} \right)^2 \right]^{1/2}. \quad (4)$$

In the previous equations, λ_{ex} is the excitation wavelength, and λ_{em} the center emission wavelength, n is the refractive index of the immersion medium (water), a is the radius of the confocal aperture divided by magnification, and w_0 and R_0 are two (generally unknown) model parameters.

When passing an excitation laser with periodically modulated polarization through a DIC prism and focusing through the objective, the resulting MDF can be approximated by:

$$U_{mod}(\mathbf{r}, t) = \varepsilon_1 \cos^2\left(\frac{\omega t}{2}\right) U\left(\mathbf{r} - \hat{\mathbf{x}} \frac{\delta}{2}\right) + \varepsilon_2 \sin^2\left(\frac{\omega t}{2}\right) U\left(\mathbf{r} + \hat{\mathbf{x}} \frac{\delta}{2}\right) \quad (5)$$

where ω is the modulation frequency, δ the shear distance of the DIC prism, $\hat{\mathbf{x}}$ is a unit vector along the x -axis perpendicular to the optical axis (z) connecting the center of the two focus positions, and the ε_1 and ε_2 are overall excitation and detection efficiency factors. When performing an FCS measurement with such a spatially modulate MDF, the resulting ACF can be calculated by:

$$g(t) = g_\infty + \frac{c}{T} \int_0^T dt_0 \int d\mathbf{r}_1 \int d\mathbf{r}_2 U_{mod}(\mathbf{r}_2, t_0 + t) \frac{1}{(4\pi Dt)^{3/2}} \exp\left[-\frac{(\mathbf{r}_1 - \mathbf{r}_2)^2}{4Dt}\right] U_{mod}(\mathbf{r}_1, t_0) \quad (6)$$

where g_∞ is the infinite lag time constant offset of the ACF, c is the concentration of fluorescing molecules, T the modulation period ($T = 2\pi/\omega$), D the diffusion coefficient, and t the lag time of the ACF. The integrations over time t_0 and over the transversal coordinates (x, y) can be carried out analytically, leading to the result:

$$g(t) = g_{\infty} + \frac{c}{4} \left[(\epsilon_1^2 + \epsilon_2^2) \left(1 + \frac{\cos \omega t}{2} \right) g_{ACF}(t) + 2\epsilon_1 \epsilon_2 \left(1 - \frac{\cos \omega t}{2} \right) g_{CCF}(t) \right] \quad (7)$$

where the autocorrelation and cross-correlation functions g_{ACF} and g_{CCF} are given by the general expression:

$$\tilde{g}(t, \delta) = \frac{c}{4} \sqrt{\frac{\pi}{Dt}} \int_{-\infty}^{\infty} dz_1 \int_{-\infty}^{\infty} dz_2 \frac{\kappa(z_1) \kappa(z_2)}{8Dt + w^2(z_1) + w^2(z_2)} \exp \left[-\frac{(z_2 - z_1)^2}{4Dt} - \frac{2\delta^2}{8Dt + w^2(z_1) + w^2(z_2)} \right] \quad (8)$$

It follows that $g_{ACF}(t) = \tilde{g}(t, 0)$ and $g_{CCF}(t) = \tilde{g}(t, \delta)$. Thus, the resulting ACF, Eq.(7), is a mixing of the functions g_{ACF} and g_{CCF} with the fast modulation terms $1 \pm \cos(\omega t)/2$.

Data fitting is performed with least-square fitting Eqs.(7) and (8) to the measured autocorrelation curve. The intrinsic fit parameters, besides constant offset and vertical scaling factor, are the diffusion coefficient D , the MDF waist parameter w_0 , and the confocal pinhole parameter R_0 . The shear distance δ of the DIC prism has to be known *a priori*. As was shown in Ref.[13], a convenient way of determining this distance is two perform a comparative measurement of the diffusion of labeled polymer beads by Dynamic Light Scattering and by 2fFCS.

3. Experiment

3.1 Materials

Atto 655 maleimide was purchased from Atto-Tec, and was dissolved in water (MilliQ, USA).

3.2 Instruments

The pmFCS setup is based on a conventional confocal microscope, as schematically shown in Figure 1. We used a linearly polarized 80MHz pulsed diode laser emitting at 635 nm (LDH-P-635, PicoQuant, Berlin, Germany). We chose to use a pulsed laser in order to compare the results of pmFCS to those of 2fFCS on the same microscope, and a cw-laser should be able to produce the same result using pmFCS. The polarization of the laser was rotated at a constant rate (100 kHz) using an electro-optical modulator (EOM, model 350-50, driver model302, Conoptics, Danbury, USA) controlled with a high-speed analog output device (PXI-6713, National Instruments, Austin, TX) programmed using Labview (National Instruments). A $\lambda/4$ waveplate was added before the EOM to improve the linearity of the beam polarization which, after the laser, shows a small ellipticity in polarization. For a perfectly linearly polarized laser beam, the $\lambda/4$ plate can be omitted. After the EOM, the light was launched into a polarization-maintaining single-mode fiber (Schäfter und Kirchhoff, Hamburg, Germany). A $\lambda/2$ waveplate was placed before the fiber to align the principal axes of the EOM to that of the fiber. The beam was re-collimated after the fiber and was then reflected by a dichroic mirror (650LP, Chroma, Rockingham, USA) into the water-immersion objective (60x, NA 1.2, Olympus, USA). A DIC (Normaski) prism was inserted in between the dichroic mirror and the objective using the conventional DIC slot of the microscope, in order to split the beam into two directions according to their polarization. We checked that the linearity of the beams' polarizations along the DIC prism axes after the dichroic mirror and before the DIC prism were $> 50:1$ with a polarization sensitive detector. After the beam was focused through the objective, two overlapping excitation foci laterally shifted by 435 nm were created (see Results), displaying anti-correlated time-dependent intensities due to the polarization modulation and polarization optics. Although aligning the beam through the EOM is not difficult, one has to make sure that the beam passes through the center of the EOM crystal. This can

be checked by proving that the beam profile is not changed by the passage through the EOM. One has also to make sure that the polarization axes of the incoming light are matching the principal axes of the EOM, as usually indicated in the EOM operation manual.

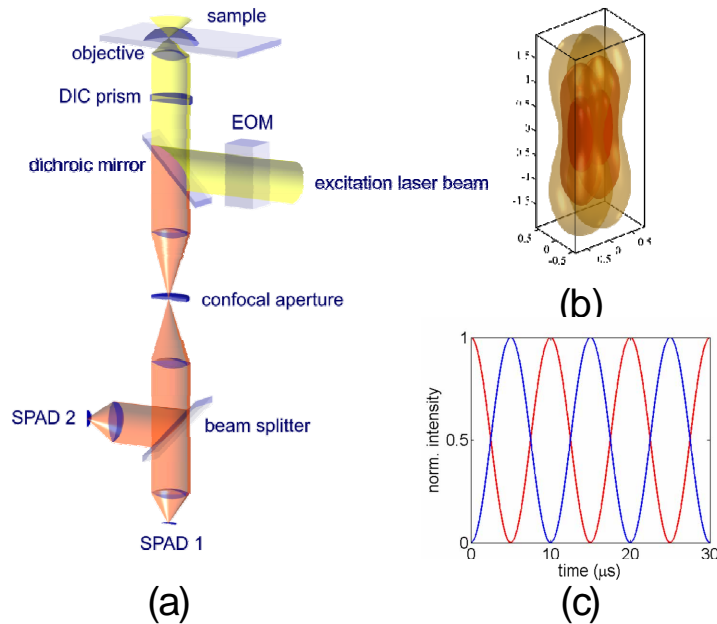


Fig. 1. (a) Schematic of the setup. Excitation is done by a single cw-laser (pulsed in the current embodiment). The polarization of the laser is periodically rotated with an EOM with $10 \mu\text{s}$ rotation period. The laser light is reflected by a dichroic beam splitter through a DIC prism. The DIC-prism deflects the laser light depending on its polarization. Thus, after focusing the light through the microscope objective, one obtains an excitation pattern which periodically swings between two laterally shifted foci. Fluorescence is collected by the same objective. The tube lens focuses the detected fluorescence from both excitation foci on a single pinhole. Subsequently, the fluorescence light is split by a 50/50 beam splitter and detected by two single photon avalanche diodes. (b) Simulation of two overlapping foci at the sample plane by exact waveoptical calculation of the excitation intensity distribution. Shown are iso-intensity surfaces for e^{-1} , e^{-2} , and e^{-3} times the maximum intensity value on optical axes in focal plane. (c) Two anti-correlated time traces at $10 \mu\text{s}$ modulation period representing the time dependent intensity of each focus.

Fluorescence was collected by the same objective, passed through the DIC prism and the dichroic mirror, and then focused through the tube lens onto a $200 \mu\text{m}$ diameter pinhole to significantly reject out-of-focus background fluorescence, while still allowing the fluorescence originating from both excitation foci to pass through. Subsequently, the fluorescence light was re-collimated, filtered using a band-pass filter and split by a non-polarizing beam splitter cube and focused onto two single-photon avalanche diodes (SPAD, SPM-AQR 14, Perkin-Elmer, Waltham, USA) by achromatic lenses. All correlation curves were generated by correlating the signals from 2 different SPADs to eliminate the artifact caused by after-pulsing. A TCSPC module measuring the arrival time of each photon from both SPADs (SPC-630, Becker & Hickl, Berlin, Germany) was used to record the detected photon arrival times. Data was analyzed by a Matlab routine provided in Supplementary Information.

The 2fFCS setup was similar to that described in detail in ref. [10] except that instead of using 2 identical lasers, the same linearly polarized pulsed diode-laser as in the pmFCS configuration was used. The pulse repetition rate was set to be 40 MHz so that the results from 2fFCS experiments are comparable with those of the pmFCS experiments. The beam was

split into orthogonal directions by a non-polarizing beam-splitter cube. One of the beams was delayed by 12.5 ns by sending it along a 3.75 meter free path, rotated in polarization by 90 degree using a $\lambda/2$ waveplate, and was recombined with the second beam using a polarizing beam-splitter cube, which recombined the split laser beam before entering the fiber. The rest of the setup was identical to the pmFCS setup.

All experiments were performed at room temperature, measured at the beginning and end of each experiment.

3. Results and discussion

To yield absolute values of diffusion coefficients (D) using pmFCS, the precise distance between two foci (δ) needs to be known. In practice, the best way to determine the precise value of δ is to perform a 2fFCS measurement on a reference dye with precisely known D . Here we chose Atto655 maleimide as the reference dye that has a diffusion coefficient of $D = 4.04 \times 10^{-6} \text{ cm}^2/\text{s}$ (Thomas Dertinger, private communication). The corresponding distance between the laser foci was fitted as 435 nm.

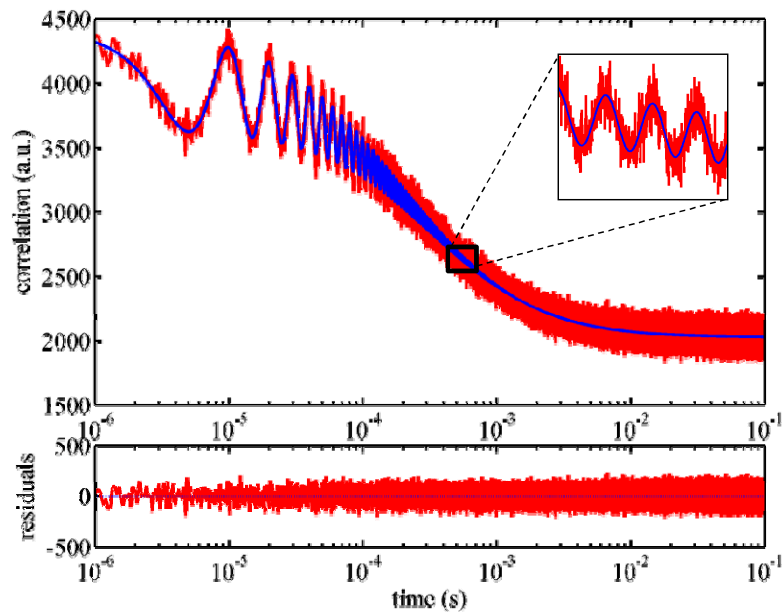


Fig. 2. pmFCS measurements on an Atto655 maleimide in aqueous solution. (Excitation power: 60 μW ; measurement time: 30 min). The autocorrelation function shows modulation in amplitude with 10 μs period, which matches the input modulation period of the excitation laser polarization. The solid line shows the fitted curve using Eq. (7). Inset shows the zoom-in of a small portion of the curve and fit. The bottom panel shows the residual of the fitting.

We performed pmFCS measurements on Atto655 maleimide in aqueous solution. A typical ACF curve and the theoretical fit are shown in Fig.2. As can be seen, the curve is a mixing of two envelope functions with a fast modulation component. Both upper and lower envelope functions are mixings of functions g_{ACF} and g_{CCF} , and the fast modulation term adopts the form $1 \pm \cos(\omega t)/2$, where ω is the modulation frequency (see Theory and Data Analysis).

It should be noted that instead of using the common multiple-tau approach [14] for generating correlation curves, in pmFCS uniform temporal resolution (100 ns) of lag times for the whole lag times as it is usually seen in multiple-tau correlation curves. This makes calculation of the ACF rather time consuming: The calculation of the ACF on a typical pentium PC

using a non-compiled Matlab routine takes a time roughly equal to the measurement time. A realistic two-parameter model (see Theory and Data Analysis and ref.[10]) rather than a 3D-Gaussian model was adopted to describe the molecular detection function (MDF) since this model has been proven to be more accurate in approximating MDF. The diffusion coefficient and the two MDF model parameters were simultaneously determined by global fitting of the complete ACF curve using the value of $\delta = 435$ nm.

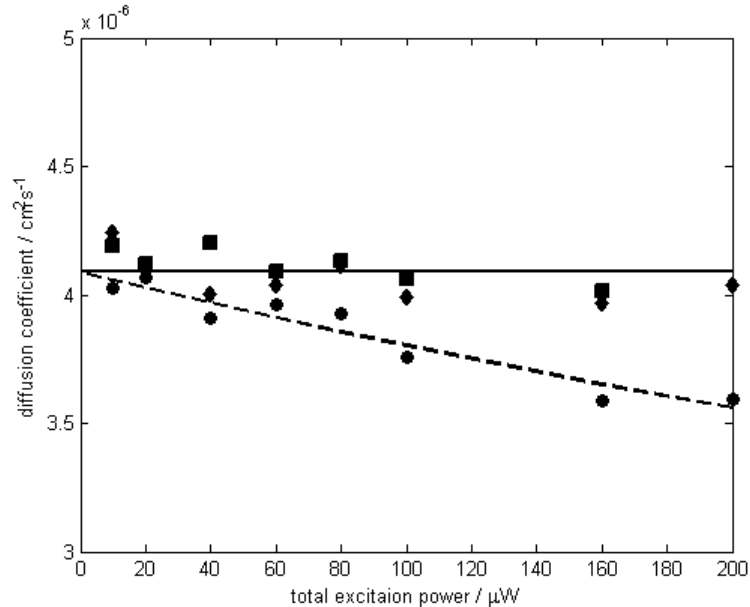


Fig. 3. Measured diffusion coefficient of Atto655 maleimide in aqueous solution at 25°C as a function of excitation power. Diffusion coefficients measured using pmFCS (squares) and 2fFCS (diamonds) are virtually independent of the excitation power up to 200 μW . The solid line is the average of these values. The results of the single-focus FCS (circles) and the second order polynomial fits (dashed line) are shown in comparison.

One advantage of 2fFCS over the conventional FCS method is its robustness against optical saturation of dyes at high excitation powers. To check whether pmFCS possesses the same robustness, and to compare pmFCS and 2fFCS methods, we measured diffusion coefficients of Atto655 maleimide at different excitation powers between 10 and 200 μW using both methods. As can be seen in Fig. 3, the conventional single focus FCS shows an apparent decrease in D upon increasing laser excitation power predicted by saturation effects, while D stays virtually constant in both 2fFCS and pmFCS experiments over the range of excitation powers used. The average of measured D for Atto655 maleimide in water corrected for 25°C equals to $(4.09 \pm 0.07) \times 10^{-6} \text{ cm}^2/\text{s}$ using pmFCS, and $(4.06 \pm 0.09) \times 10^{-6} \text{ cm}^2/\text{s}$ using 2fFCS. These two values agree with each other within the measurement error (standard deviation), and both agree reasonably well with the reference value with $< 2\%$ error. It should be mentioned that no photobleaching was observed over the range of excitation power used here, whether in 2fFCS or in pmFCS experiments, which would have become visible as an increasing D with increased excitation intensity. Compared to ref.[10], this could be explained by the slightly larger foci in our setup, resulting in a reduced local intensity.

An important parameter for the accuracy of pmFCS (and generally 2fFCS) is the perfection of beam polarization. As stated above, the polarization ratio was checked to be better than 50:1, leading to a residual bleed through of 2 % of the “wrong” polarization and potentially introducing a systematic error. However, because we use the same measurement sys-

tem and the known diffusion of a reference dye for calibrating the distance δ between foci, this should cancel out any residual error stemming from imperfect polarization.

4. Conclusion

We demonstrated a new technique based on the established 2fFCS method. This new technique possesses the same ability to measure the absolute value of diffusion coefficient of diluted fluorescent solution samples as the 2fFCS method. The fundamental reason behind the success of these two techniques is the introduction of an external ruler for the absolute distance needed to obtain the absolute diffusion coefficient. It has also been shown that, as with the 2fFCS technique, the new technique is also robust against optical saturation in producing the correct diffusion coefficient in contrast to conventional FCS (where diffusion coefficient decreases at high excitation power due to optical saturation). Compared to the 2fFCS setup, pmFCS is simpler and cheaper to implement and more compatible with the conventional confocal microscope setup using cw-excitation. It only requires the addition of an EOM, a DIC prism and a few extra mirrors to a conventional confocal setup. Of course, the method can reliably measure diffusion processes with characteristic diffusion times that are by roughly by one order of magnitude slower than the polarization modulation period (here 10 μ s). For most studies on protein diffusion, the modulation period used in the present is short enough, but in case one would like to study faster diffusion processes, it will be straightforward to increase the modulation frequency by using faster EOMs.

Acknowledgement

J.E. gratefully acknowledges financial support by the Deutsche Volkswagenstiftung. Y.K. and T.D. thank the National Institute of Health for the financial support by grant GM069709-01 to S.W.